Available online at www.sciencedirect.com
ScienceDirect
Journal of Power Sources 165 (2007) 267–278
JOURNAL OF POWER SOURCES
www.elsevier.com/locate/jpowsour

A Bayesian network fault diagnostic system for proton exchange membrane fuel cells

Luis Alberto M. Riascos [a,*], Marcelo G. Simoes [b], Paulo E. Miyagi [c]

[a] *Federal University of ABC, r. Santa Adelia, 166, CEP 09210-170, Santo Andre, SP, Brazil*
[b] *Colorado School of Mines, 1500 Illinois Street, 80401, Golden, CO, USA*
[c] *Escola Politecnica, University of Sao Paulo, Av. Prof. Mello Moraes, 2231, CEP 05508-900, Sao Paulo, Brazil*

Received 1 November 2006; received in revised form 4 December 2006; accepted 5 December 2006
Available online 10 January 2007

Abstract

This paper considers the effects of different types of faults on a proton exchange membrane fuel cell model (PEMFC). Using databases (which record the fault effects) and probabilistic methods (such as the Bayesian-Score and Markov Chain Monte Carlo), a graphical–probabilistic structure for fault diagnosis is constructed. The graphical model defines the cause-effect relationship among the variables, and the probabilistic method captures the numerical dependence among these variables. Finally, the Bayesian network (i.e. the graphical–probabilistic structure) is used to execute the diagnosis of fault causes in the PEMFC model based on the effects observed.

Keywords: Bayesian networks; Fault diagnosis; Fuel cells

1. Introduction

Environmental issues have increased the demand for less polluting energy generation technologies. Governmental actions to support a hydrogen-based economy are under way, as well. Most recent developments in proton exchange membrane fuel cell (PEMFC) technology have made them commercially available for stationary and mobile applications in the range of up to 200 kW.

Fuel cells (FCs) convert the energy contained in hydrogen directly into electricity with only water and heat as the products of the reaction. Under certain pressure, hydrogen (H_2) is supplied into a porous conductive electrode (the anode). The H_2 spreads through the electrode until it reaches the catalytic layer of the anode, where it reacts to form protons and electrons. The H^+ ions (or protons) flow through the electrolyte (a solid membrane), and the electrons pass through an external electrical circuit, producing electrical energy. On the other side of the cell, the oxygen (O_2) spreads through the cathode and reaches its catalytic layer. On this layer, the O_2, H^+ protons, and electrons produce liquid water and residual heat as sub-products [5].

Several papers have been published considering FC operation in normal conditions; but only few of them addressed the FC operation under fault analysis. Faults are events that cannot be ignored in any real machines, and their consideration is essential for improving the operability, flexibility, and autonomy of commercial equipment.

In this paper, Bayesian network algorithms are applied for the construction of a graphical–probabilistic structure to fault diagnosis in PEMFCs.

This paper is organized as follows. In Section 2, the basic concepts for the mathematical model of a PEMFC are introduced. In Section 3, four types of faults in PEMFC are considered: faults in the air fan; faults in the refrigeration system; growth of the fuel crossover; and faults in the hydrogen pressure. Section 4 introduces a short background of Bayesian networks and learning algorithms to apply on fault diagnosis of PEMFC.

2. The fuel cell model

A mathematical model of a fuel cell (FC) was used to study the possible fault effects. This model consists of an electro-chemical and a thermo-dynamical sub-model.

* Corresponding author. Tel.: +55 11 49963166; fax: +55 11 30915471.
E-mail address: luis.riascos@ufabc.edu.br (L.A.M. Riascos).

0378-7753/$ – see front matter © 2006 Elsevier B.V. All rights reserved.
doi:10.1016/j.jpowsour.2006.12.003

2.1. The electrochemical model

The output voltage V_{FC} of a single cell can be defined as the result of the following expression [11]:

$$V_{FC} = E_{Nernst} - V_{act} - V_{ohmic} - V_{con} \quad (1)$$

E_{Nernst} is the thermodynamic potential of the cell representing its reversible voltage:

$$E_{Nernst} = 1.229 - 0.85 \times 10^{-3}(T - 298.15) + 4.31 \times 10^{-5} T \left[\ln(P_{H_2}) + \frac{1}{2}\ln(P_{O_2})\right] \quad (2)$$

where: P_{H_2} and P_{O_2} (atm) are the hydrogen and oxygen pressures, respectively, and T (K) is the operating temperature.

V_{act} is the voltage drop due to the activation of the anode and the cathode:

$$V_{act} = -[\xi_1 + \xi_2 T + \xi_3 T \ln(c_{O_2}) + \xi_4 T \ln(I_{FC})] \quad (3)$$

where ξ_i ($i = 1$–4) are specific coefficients for every type of FC, I_{FC} (A) is the electrical current, and c_{O_2} (atm) is the oxygen concentration.

V_{ohmic} is the ohmic voltage drop associated with the conduction of protons through the solid electrolyte, and of electrons through the internal electronic resistance:

$$V_{ohmic} = I_{FC}(R_M + R_C) \quad (4)$$

where R_C (Ω) is the contact resistance to electron flow, and R_M (Ω) is the resistance to proton transfer through the membrane:

$$R_M = \frac{\rho_M \ell}{A},$$

$$\rho_M = \frac{181.6[1 + 0.03(I_{FC}/A) + 0.062(T/303)^2 (I_{FC}/A)^{2.5}]}{[\psi - 0.634 - 3(I_{FC}/A)] \exp[4.18(T - 303/T)]} \quad (5)$$

where ρ_M (Ω cm) is the specific resistivity of membrane, ℓ (cm) is the thickness of membrane, A (cm^2) is the active area of the membrane, and ψ is a coefficient for every type of membrane.

V_{con} represents the voltage drop resulting from the mass transportation effects, which affects the concentration of the reacting gases:

$$V_{con} = -B \ln\left(1 - \frac{J}{J_{max}}\right) \quad (6)$$

where B (V) is a constant depending on the type of FC, J_{max} is the maximum electrical current density, and J is the electrical current density produced by the cell. In general, $J = J_{out} + J_n$ where J_{out} is the real electrical output current density, and J_n is the fuel crossover and internal loss current.

Considering a stack composed by several FCs, and as first order analysis, the output voltage is $V_{Stack} = nr V_{FC}$, where nr is the number of cells composing the stack. However constructive characteristic of the stack such as flow distribution and heat transfer should be taken [1,10,19].

In this paper, a mathematical model for a 500 W stack (manufactured by BCS Technologies) is used. The parameters for this particular model are presented in Table 1. In [6] the polarization curve obtained with this model is compared to the polarization curve of the manufacturing data sheet to validate the model.

Table 1
Parameters of a PEMFC BCS, 500 W

Parameter	Value
nr	32
A	64 cm^2
ℓ	178 μm
P_{O_2}	0.2095 atm
P_{H_2}	1 atm
R_C	0.003 Ω
B	0.016 V
ξ_1	−0.948
ξ_2	$0.00286 + 0.0002 \ln A + (4.3 \times 10^{-5}) \ln c_{H_2}$
ξ_3	7.6×10^{-5}
ξ_4	-1.93×10^{-4}
ψ	23.0
J_n	3 mA cm^2
J_{max}	0.469 A cm^2

In general, these parameters are based on manufacturing data and laboratory experiments, and their accuracy can affect the simulation results. In [5], a multi-parametric sensitivity analysis is performed to define the importance of the accuracy of each parameter. Basically, the parameters are classified in three groups: insensitive (A, R_C, ℓ), sensitive (J_n, B, ψ, ξ_4), and highly sensitive parameters (J_{max}, ξ_3, ξ_1). The accuracy was analyzed in normal conditions, considering variations around ±10% of their normal values. However, in fault conditions, those variations can be stronger, as presented in Sections 3.1–3.4.

2.2. The thermo-dynamical model

The calculation of the relative humidity and the operating temperature of the FC essentially compose the thermo-dynamical model [7].

2.2.1. Temperature

The variation of temperature is obtained with the following differential equation:

$$\frac{dT}{dt} = \frac{\Delta \dot{Q}}{M C_s} \quad (7)$$

where M (kg) is the whole stack mass, C_s (J K^{-1} kg^{-1}) is the average specific heat coefficient of the stack, $\Delta \dot{Q}$ (J s^{-1}) is the rate of heat variation (i.e. the difference between the rate of heat generated by the cell operation ($\dot{Q}_{gen}$) and the rate of heat removed). Heat can be removed by the air flowing inside the stack ($\dot{Q}_{rem_1}$), by the refrigeration system ($\dot{Q}_{rem_2}$), by water evaporation ($\dot{Q}_{rem_3}$), and by heat exchanged with the surroundings ($\dot{Q}_{rem_4}$).

In this FC system, the refrigeration system is turned on when the operating temperature is higher than 50 °C.

2.2.2. Relative humidity

A correct level of humidity should be maintained in the FC. This level is measured through the relative humidity HR. The relative humidity HR_{out} of the output air is calculated from the equation:

$$HR_{out} = \frac{P_{W_{in}} + P_{W_{gen}}}{P_{sat\_out}} \quad (8)$$

where $P_{W_{in}}$ is the partial pressure of the water in the inlet air; $P_{W_{gen}}$ is the partial pressure of the water generated by the chemical reaction [11]; P_{sat_out} is the saturated vapor pressure in the output air. Considering that $HR_{out} \times P_{sat\_out} = P_{W\,out}$, Eq. (8) establishes the balance of water: output = input + internal generation.

The P_{sat} is calculated from the equation:

$$P_{sat} = T^a \exp\frac{(b/T + c)}{10}$$

If $T > 273.15$ (°K), then $a = -4.9283$; $b = -6763.28$; $c = 54.22$;

If the HR is much smaller than 100%, then the membrane dries out and the conductivity decreases. On the other hand, a relative humidity greater than 100% produces accumulation of liquid water on the electrodes, which can become flooded and block the pores; this makes gas diffusion difficult. The result of these two conditions is a fairly narrow range of normal operating conditions. In conclusion the ideal operational condition is HR = 100%. In this equipment, the control system adjusts the air-reaction volume to maintain the HR close to 100%. In [16] this control technique has been implemented.

In abnormal conditions some parameters change, i.e. flooding and drying condition affects R_C and R_M, respectively. Also in [9] the variation of the resistances had been associated with fault detection of flooding and drying.

Fig. 1 (adapted from [11]) illustrates the variation of temperature and relative humidity for different stoichiometry air relationships ($\lambda = 2, 4$). The stoichiometry λ is the relationship between inlet air divided by the air necessary for the chemical reaction. In general, the maximum efficiency occurs at about 80% of fuel utilization (H_2) and 50% of oxygen utilization. Therefore, for a good concentration of O_2 in the air through the entire FC, λ should be bigger than 2 [11].

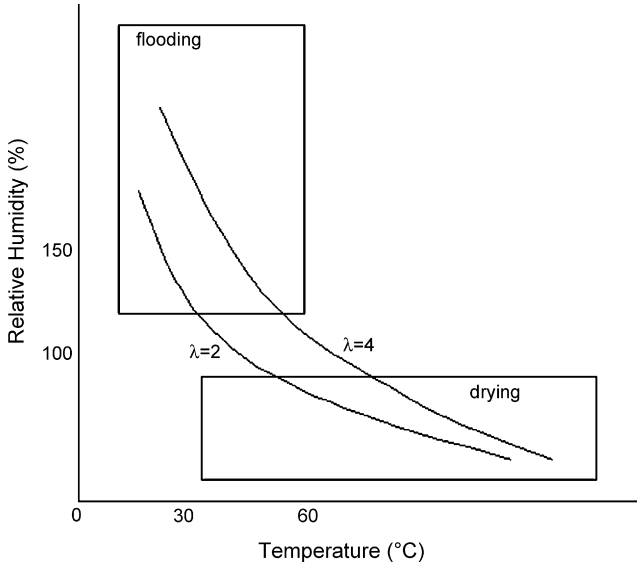

Fig. 1. Temperature and relative humidity for $\lambda = 2, 4$ (adapted from [11]).

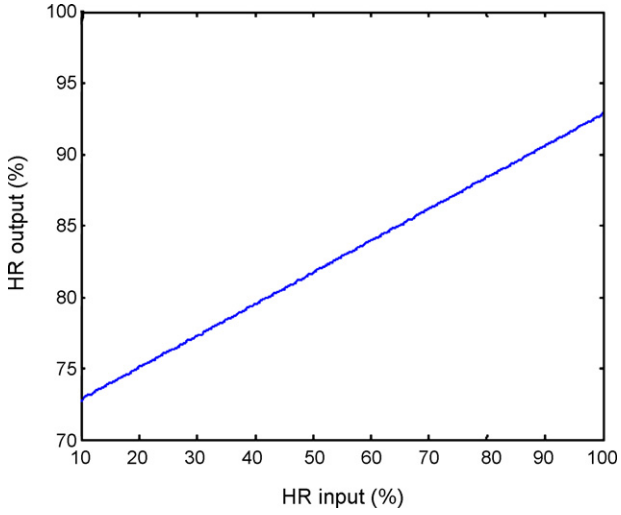

Fig. 2. Variation of output HR vs. input HR.

To prevent the membrane from drying, some researchers (e.g. [11]) have proposed extra humidification on the input air. However, the variation in the HR of the input air produces a very small adjustment in the output HR; for example, a variation of 10% on the input HR represents a variation of approximately 2% on the output HR. Thus, in many cases, the extra humidification of the input air is not enough to resolve the drying problem. Fig. 2 illustrates the variation produced on the HR of output air by the adjustment in the HR of input air.

2.3. Normal operation of a fuel cell

Fig. 3 illustrates the evolution of a few PEMFC variables in normal operating conditions as a function of time. The variables are: voltage$_{stack}$ (V), electrical current I_{FC} (A), temperature (°C), volume of air flow (L s^{-1}), and stoichiometry air relationship λ. In this test, the FC supports a constant-load demand; thus, the voltage and current should vary by themselves to maintain this demand (i.e. the output power would be constant). Also the control system adjusts the air-reaction volume to maintain the HR close to 100%.

The simulation begins with the FC system in stand-by (i.e. without load, and at environmental temperature, approximately 25 °C). After the load requirement, the electrical equilibrium is reached in less than 3 s (e.g. the equilibrium of voltage and current). On the other hand, the temperature begins to increase until, at $t = 10$ min, it reaches 50 °C. Then, the refrigeration system is turned on. The temperature increases slowly until the thermo-dynamical steady state is reached after $t = 40$ min. Note that variations on the temperature have influenced the evolution in the airflow and λ. Also, variations in voltage and current are performed, especially in the first 10 min, but they are produced by a slower evolution of the thermo-dynamical state.

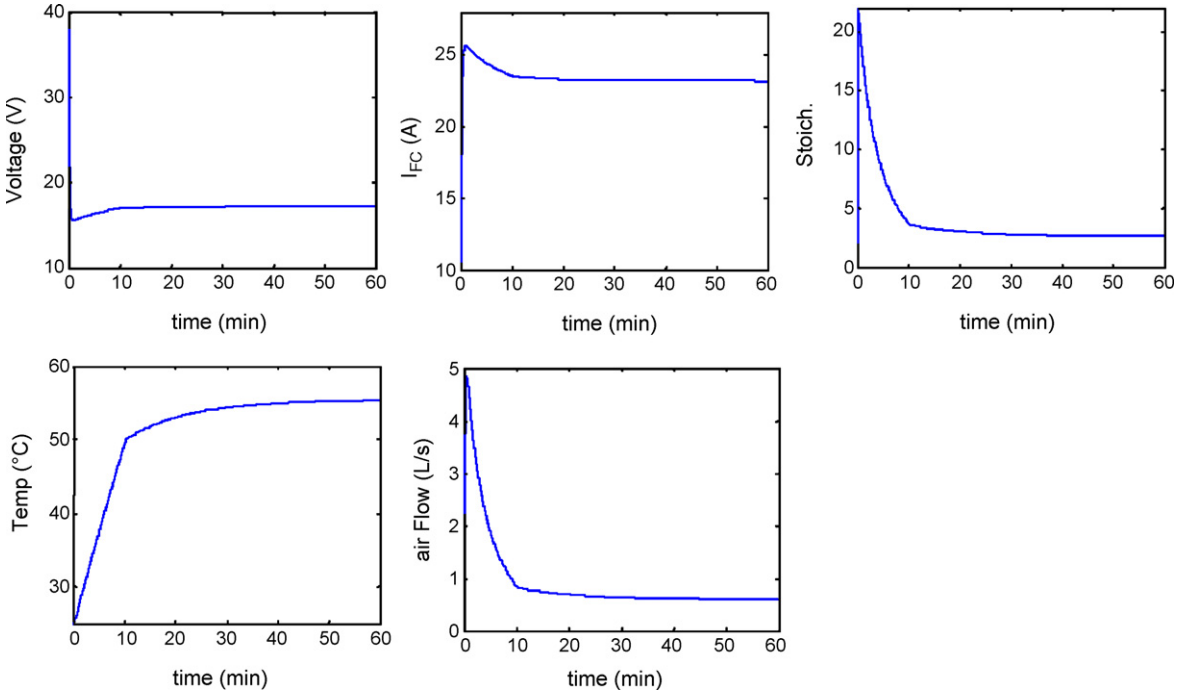

Fig. 3. Evolution of variables of a FC in normal conditions deriving from a mathematical model in MATLAB®.

3. Faults in fuel cells

In general, two types of fault detection can be considered:

- Faults that can be detected by monitoring a specific variable. For example, the leak of fuel can be detected by installing a specific gas sensor. In this case, a diagnosis is not necessary.
- Faults that cannot be detected directly by monitoring or faults that need some type of diagnosis.

Usually, fault detection on commercial fuel cell equipment is limited to detection of faults of the first type. This work focuses on fault detection of the second type.

Four types of faults in PEMFCs are considered in this study: (1) fault in the air fan, (2) fault in the refrigeration system, (3) growth of the fuel crossover, and (4) fault in the hydrogen pressure. The effects of these faults are included in the mathematical model to analyze the behavior of the FC system in fault operation conditions.

3.1. Fault in the air reaction fan

A reduction of the reaction air by a fault in the air fan can produce two major effects: (1) accumulation of liquid water than cannot be evaporated and (2) reduction of O_2 volume below that necessary for a complete reaction with the H_2.

A common method for removing excess water inside the FC is using the air flowing through it. The correct variation of the stoichiometry λ maintains the HR proximal to 100%. However, when a fault in the air fan takes place, this becomes impossible. This fault reduces the air reaction flow, which reduces the water evaporation volume and permits the accumulation of water. A great accumulation of water causes the flooding of electrodes making gas diffusion difficult and affecting the performance of the FC. These effects are simulated by Eq. (9), which was obtained empirically.

$$\mathrm{Rc}_{(k)} = \mathrm{Rc}_{(0)} \cdot \left(\frac{w_{\mathrm{acum}(k)}}{\mathrm{const}_1} \right)^{0.8}, \quad J_{\max(k)} = \frac{J_{\max(0)}}{(w_{\mathrm{acum}(k)}/\mathrm{const}_1)^{1.2}} \tag{9}$$

where $J_{\max(0)}$ is the value of the maximum electrical current density at the initial state (normal condition), $\mathrm{Rc}_{(0)}$ is the value of the variable at the initial state (normal condition), $w_{\mathrm{acum}(k)}$ is the volume of water accumulated at instant k, and const_1 is a constant defining when the electrodes are led to flooding.

The second effect of a fault in the air fan occurs when λ is below the practical and recommended value. In this case, the O_2 concentration is reduced and the exit air completely depleted of O_2. This reduction of O_2 concentration produces a negative effect on the E_{Nernst} (Eq. (2)) and increase on the V_{act} (Eq. (3)). In this case, the O_2 concentration changes according to empirical Eq. (10):

$$c_{\mathrm{O}_{2(k)}} = \frac{c_{\mathrm{O}_{2(0)}}}{\sqrt{\mathrm{const}_2/\lambda_{(k)}}} \tag{10}$$

where $c_{\mathrm{O}_{2(k)}}$ is the O_2 concentration at instant k, $c_{\mathrm{O}_{2(0)}}$ is the normal O_2 concentration in the air, and const_2 is a constant defining when λ is lower than necessary for the chemical reaction.

Fig. 4 illustrates the evolution of a few variables when a fault in the air fan is considered. The variables are $\mathrm{voltage}_{\mathrm{stack}}$ (V), I_{FC} (A), temperature (°C), air flow ($\mathrm{L\,s^{-1}}$), λ, and accumulated water (L). In this case, the starting point of the simulation

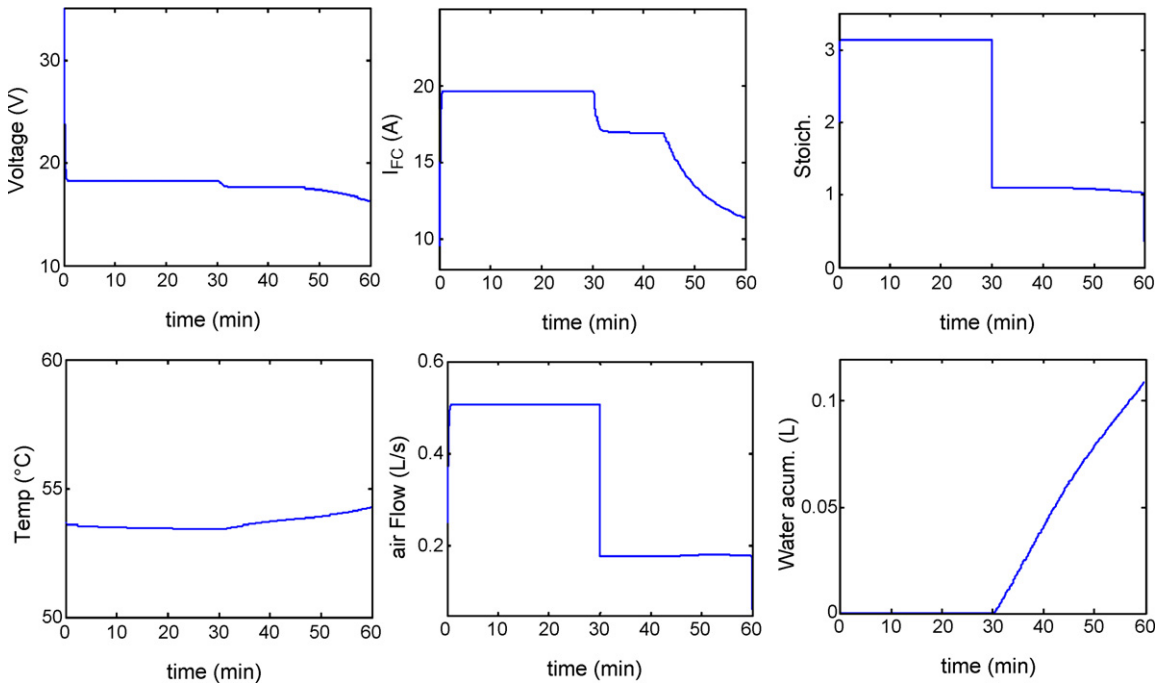

Fig. 4. Evolution of variables by fault in the reaction air fan.

($t=0$) is an FC on thermal steady state. The fault in the air fan takes place at $t=30$ min. The initial effect is the variation of the airflow volume, which reduces λ close to 1, affecting voltage and I_{FC}. Also, this fault produces accumulation of liquid water and, at $t=45$ min, the accumulation of water is enough to produce variation on the resistance of electrodes affecting voltage and I_{FC} continuously.

3.2. Fault in the refrigeration system

The refrigeration system maintains temperature within the normal operating conditions. When the temperature increases, the reaction air has a drying effect and reduces the relative humidity HR. A low HR can produce a catastrophic effect on the polymer electrolyte membrane, which not only totally relies upon high water content, but is also very thin (and thus prone to rapid drying out). The drying of the membrane changes the resistance of membrane to proton flow (R_M, Eq. (4)). R_M is affected by the adjustment of ψ (Eq. (5)), which varies according to empirical equation (11):

$$\psi_{(k)} = \frac{\psi_{(0)}}{(\text{const}_3/\text{HR}_{\text{out}(k)})^{1.12}} \tag{11}$$

where, const_3 defines when the membrane is led to drying.

The variation of R_M produces an increase in the ohmic voltage drop V_{ohmic}, equation (4), and it produces the reduction of V_{FC}, Eq. (1).

Fig. 5 illustrates the evolution of the variables $\text{voltage}_{\text{stack}}$ (V), I_{FC} (A), temperature (°C), air flow (L s^{-1}), λ, and heat removed by the refrigeration system $\dot{Q}_{\text{rem}_2}$ (W), when a total fault in the refrigeration system is considered at $t=30$ min.

The initial fault effect (at $t=30$ min.) is the increase in temperature. Then, the FC controller automatically reduces λ, maintaining the performance of the FC. However, when $\lambda=2$ (i.e. the minimum value recommended) is not further reduced, and then the drying effect has a continuous influence on the $\text{voltage}_{\text{stack}}$, I_{FC}, air flow and other variables.

3.3. Increase of fuel crossover (J_n)

There is a small amount of wasted fuel that migrates through the membrane. It is defined as fuel crossover—some hydrogen will diffuse from the anode (through the electrolyte) to the cathode, react directly with the oxygen, and produce no current for the FC.

In normal conditions, the flow of fuel through the membrane (J_n) is very small, typically representing only a few mA cm^2. A sudden increase in this variable can be associated with rupture of membrane.

This variation of J_n produces an increase in the concentration voltage drop (V_{con} Eq. (6)), and therefore a reduction of V_{FC}, Eq. (1).

Fig. 6 illustrates the evolution of the variables $\text{voltage}_{\text{stack}}$ (V), I_{FC} (A), temperature (°C), air flow (L s^{-1}), and λ, when a sudden variation of J_n is performed from 0.003 to 0.1 A cm^2 at $t=30$ min.

The initial effect is a variation on all the variables including the power produced by the FC. The FC controller automatically adjusts the stoichiometry (by reducing the airflow) until, at $t=47$ min, it reaches $\lambda=2$, and then cannot be further reduced. This affects the output HR and other variables.

3.4. Fault in the hydrogen feed line

In general, for mobile and stationary applications, the hydrogen is supplied from a high-pressure bottle and reduced by a

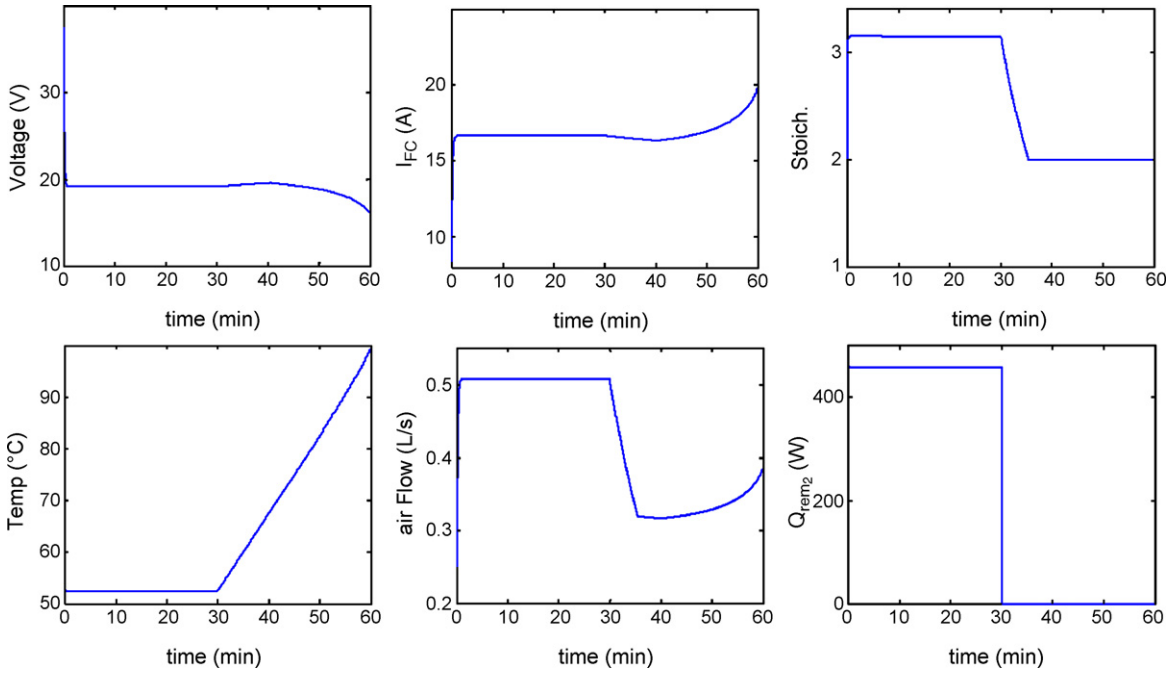

Fig. 5. Evolution of variables by fault in the refrigeration system.

pressure controller. In normal conditions, the hydrogen pressure is assumed to be constant (1 atm). Variation in the hydrogen pressure affects the performance of the FC. A lower pressure negatively affects the performance of the FC. The reduction of H_2 pressure reduces the density of current J affecting I_{FC}, decreases E_{Nernst} equation (2), increases V_{act} equation (3), and has a corresponding effect on V_{FC}, equation (1).

Fig. 7 illustrates the evolution of the variables voltage$_{stack}$ (V), I_{FC} (A), temperature (°C), air flow (L s^{-1}), λ, and H_2 pressure (atm), when a reduction on the H_2 pressure is considered from 1 to 0.2 atm at $t = 30$ min.

Fault in the oxygen feed line (such as a fault produced by blocking the air filter), can be an interesting issue in a fault-tolerant FC system. In practical applications, the oxygen is supplied from the air where it has a constant pressure. Therefore, a fault in the air reaction feed line does not produce a variation in the air (or oxygen) pressure; instead, a reduction on the O_2 concentration can be produced. However, the effects

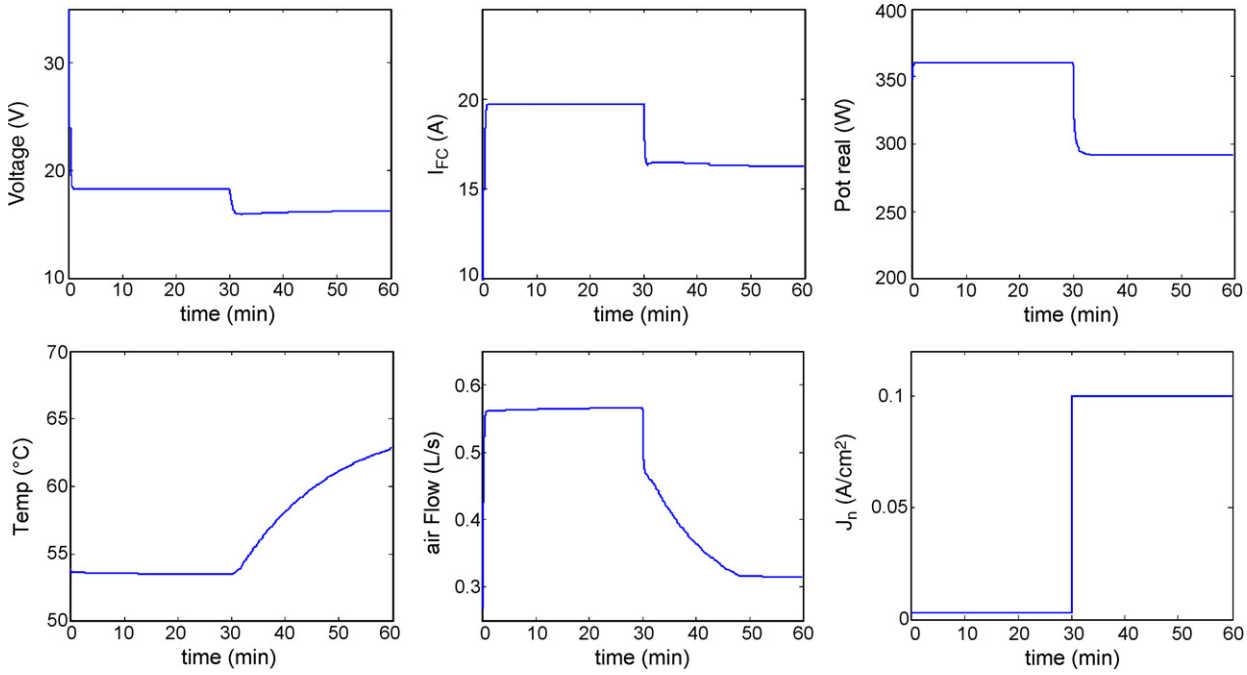

Fig. 6. Evolution of variables by increasing J_n.

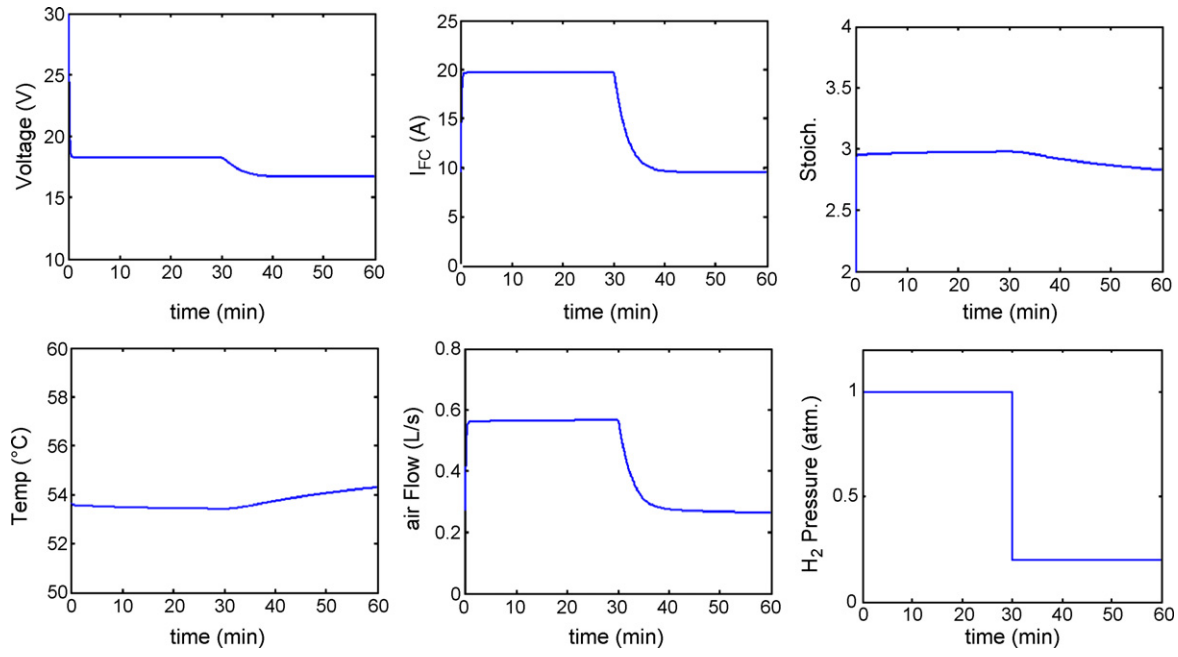

Fig. 7. Evolution of variables by reduction in H_2 pressure.

of this fault are similar to a fault in the air reaction fan (see Section 3.1).

In Section 3, the effects of four types of faults on the FC operation were explained simply and directly. But, when a fault happens, an interconnected dependence among the variables is performed. That makes diagnosis of the fault cause difficult. Figs. 4–7 illustrate this dependence where, in all cases of faults, all the variables have performed changes.

By implementing those types of faults, and their effects, on the mathematical model of the FC, databases for recording the evolution of variables in fault conditions can be constructed. Then, probabilistic approaches can be applied on the databases to qualify and quantify the dependency relationship among the variables. In the next section, Bayesian networks are considered for the construction of a graphical–probabilistic structure based on databases.

4. Bayesian networks for fault diagnosis

Bayesian networks have been extensively applied to fault diagnosis, e.g. [12] and [3]; however, in the area of fuel cells, it is a new field. In [12], a Bayesian network is implemented for controlling an unsupervised fault tolerant system to generate oxygen from the CO_2 on Mars atmosphere. In [3], Bayesian network is applied for fault diagnosis in a power delivery system. One advantage of Bayesian network is that it allows the combination of expert knowledge of the process and probabilistic theory for the construction of a diagnostic procedure; nevertheless, both are recommended for the construction of a "good" Bayesian network.

A Bayesian network is a structure that graphically models relationships of probabilistic dependence within a group of variables. A Bayesian network $B = (\mathcal{G}, CP)$ is composed of the network structure and the conditional probabilities (CP). A directed acyclic graph (DAG) represents the graphical structure $\mathcal{G}$, where each node of the graph is associated to a variable X_i, and each node has a set of parents $pa(X_i)$. The conditional probabilities CP, numerically capture the probabilistic dependence among the variables [2].

The construction of a graph to describe a diagnostic process can be executed in two ways:

- Based on human knowledge about the process, where relationships among variables are established to define the criteria for choosing the next state (i.e. the relationship between variables and parents);
- Based on probabilistic methods using databases of records.

The construction of a Bayesian structure $\mathcal{G}$ based on knowledge can be relatively simple; but its efficacy depends completely on the human expert knowledge about that domain.

The implementation of probabilistic methods for the structure learning can follow two approaches: constraint-based and search-and-score. In the constraint-based approach, the starting point is an initially given graph $\mathcal{G}$. And then, edges are removed or added if certain conditional independencies are measured in the database. In the search-and-score approach, a search through the space of possible DAGs is performed for finding for the best DAG. In this research, the Bayesian-score (K2) [4] and Markov chain Monte Carlo (MCMC) [14] algorithms are applied. The K2 and MCMC algorithms are relatively easy to be applied on an automatic generation of the graph, and they are already implemented in the MatLab BNToolbox [13].

The number of DAGs, as a function of the number of nodes ($f(n)$), grows exponentially with n. According to [4], a recursive function can be used to know the number of DAGs as function

of the number of variables:

$$f(n) = \sum_{i=1}^{n} (-1)^{i+1} \left(\frac{n}{i}\right) 2^{i(n-i)} f(n-i) \quad (12)$$

For example, a model with 16 variables ($n = 16$) has 8.38×10^{46} possible DAGs. Thus, an exhaustive search on the space of all DAGs is not practical. Therefore, a local (e.g. K2) or a stochastic (e.g. MCMC) search should be made.

In this work, the construction of a Bayesian network for fault diagnosis begins with the generation of a graph applying probabilistic methods and, after that, refined using constrains and domain knowledge. The complete sequence consists of the following steps:

1. Construction of the database—the records are provided from a mathematical model of a PEMFC implemented on MatLab®. Field experiments could also provide those records as considered in [16]; however, two major problems are pointed out: (a) a large amount of data is necessary where the generation of each case takes around 2 h of supervised experiments, and (b) variables such as Q_{gen}, flooding, λ, etc, impose additional challenges to be monitored.
2. Implementation of search-and-score algorithms (K2 and MCMC) to find the initial structure. The probabilistic approaches were implemented using the BNT (Bayesian Network Toolbox) developed for MatLab® [13].
3. Constraint-based conditions and knowledge are applied for improving the structure.
4. Calculation of conditional probabilities. The conditional probabilities are calculated on the resulting structure.

4.1. Database generation

In this research, the diagnosis is executed at a specific moment, only if abnormal evolution of any variable is monitored; the idea is to associate this evolution with symptoms of incipient faults. Then binary states of the variables are generated (0 = normal, 1 = abnormal). The general procedure is to monitor a specific variable; if after a fault takes place and the value of such variable is off a certain tolerance band, then a flag should be turned to "1". Fig. 8 represents the range of tolerance of the I_{FC} and the evolution after a fault at $t = 30$ min.

The next step is the construction of a vector containing the value of all variables. This vector corresponds to a single case in the database with values of all variables in a certain period.

From the mathematical model, the evolution of variables that can be difficult to monitor on a real machine (such as Q_{gen} or HR) can be observed. Records of all variables are essential for the construction of the network structure avoiding hidden variables.

The variables considered are the following:

J_n = fault by fuel crossover
aF = fault in the air fan
rF = fault in the refrigeration system
H_2 = fault by low H_2 pressure

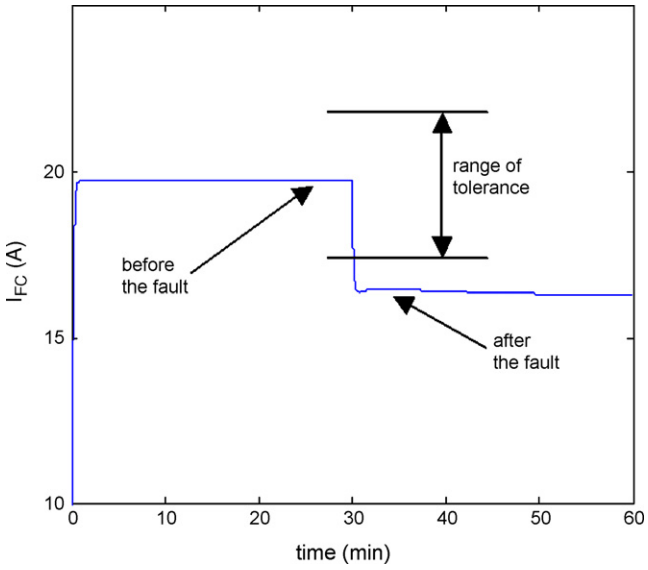

Fig. 8. Evolution of I_{FC} by a fault at $t = 30$ min.

Flow = volume of air flow
Q_{gen} = generated heat
LL = stoichiometry air relationship λ
HR_{out} = output relative humidity
Drying = drying of membrane
Flood = flooding of electrodes
Ov = overload (i.e. the FC is working close to the maximum load; in those cases, same variables can perform a different evolution)
Volt = $voltage_{stack}$
$I = I_{FC}$ electrical current of the FC
T = temperature
Power = difference between real output power and required load
$pH_2 = H_2$ pressure

A database with 10,000 cases was constructed for the structure learning of a Bayesian network for fault diagnosis in fuel cells. The database considers different operational conditions with different fault causes simulated and, selected in a random sequence.

A vector for fault diagnosis in FC has the structure presented in Fig. 9.

4.2. The Bayesian-score (K2) algorithm

The K2 algorithm [4] is a very useful search algorithm. Initially, each node has no parents. It then incrementally adds those parents, the addition of which increases the score of the resulting structure even more. When the addition of no single parent increases the score, it stops adding parents to the node. Before the algorithm begins, the possible parents of every variable must be defined. Therefore, the human-expert experience is important to define that order. If the order is known, a search over this order is more efficient than searching over all DAGs. The K2 algorithm

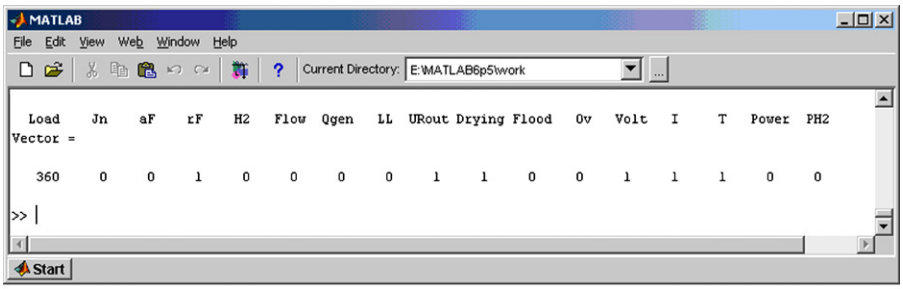

Fig. 9. Generation of a vector for the construction of the database.

maximizes the next function:

$$P(\mathcal{G}|D) = P(B_s)\prod_{i=1}^{n}\prod_{j=1}^{q_i}\frac{(r_i-1)!}{(N_{ij}+r_i-1)!}\prod_{k=1}^{r_i}N_{ijk}!, \tag{13}$$

where N_{ijk} is the number of occurrences of $\{X_i = x_{ij}|\ \mathrm{pa}(X_i) = \pi_{ik}\}$, r is the number of values of X_i, q is the number of values of $\mathrm{pa}(X_i)$, and n is the number of variables. x_{ij} and π_{ik} are specific values of the variable X_i and $\mathrm{pa}(X_i)$. $P(\mathcal{G}|D)$ is the score of the DAG $\mathcal{G}$ to represent the database D.

Fig. 10 illustrates the resulting network structure applying the K2 algorithm. The order of the variables follows:

$J_n = 1$, aF = 2, rF = 3, $H_2 = 4$, Flow = 5, $Q_{gen} = 6$, LL = 7, Flood = 8, Drying = 9, $HR_{out} = 10$, Ov = 11, Volt = 12, $I = 13$, $T = 14$, Power = 15, $pH_2 = 16$.

For example, according to Fig. 10, a probabilistic dependence between variable 1 (as parent) and variables {2, 3, 4, 6, 9 and 11} (as children) is established from the database.

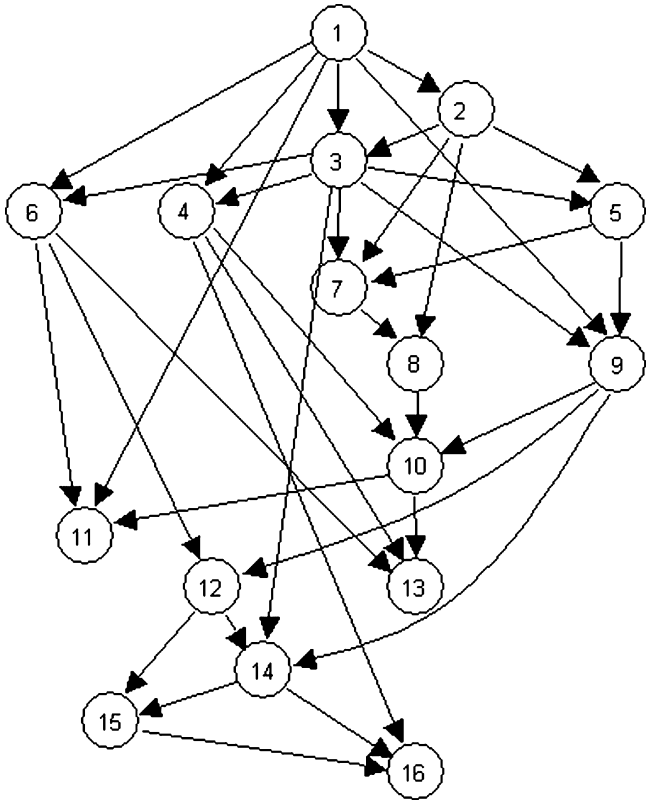

Fig. 10. Bayesian network structure implementing the K2 algorithm.

4.3. The MCMC (Markov Chain Monte Carlo) algorithm

The MCMC algorithm is composed of a Markov Chain and a Monte Carlo process. A Markov Chain is a stochastic process, where the current state depends only on the past state. Applying a Markov Chain in Bayesian networks, the chain is the sequence of DAGs in which the search for the best DAG is performed.

A Monte Carlo is a probabilistic approximation for a very complex, or unknown function. The Monte Carlo process finds a very complex function (i.e. the DAG) that best agreed with the evidence contained in the database by applying a probabilistic approximation.

The MCMC algorithm starts at a specific point in the space of DAGs. The search is performed through all the nearest neighbors, and it moves to the neighbor that has the highest score. If no neighbor has a higher score than the current point, a local maximum has been found and the algorithm stops. A neighbor is the graph that can be generated from the current graph by adding, deleting or reversing a single arc.

Fig. 11 illustrates the resulting network structure applying the MCMC algorithm where the variable order is the same as in Fig. 10.

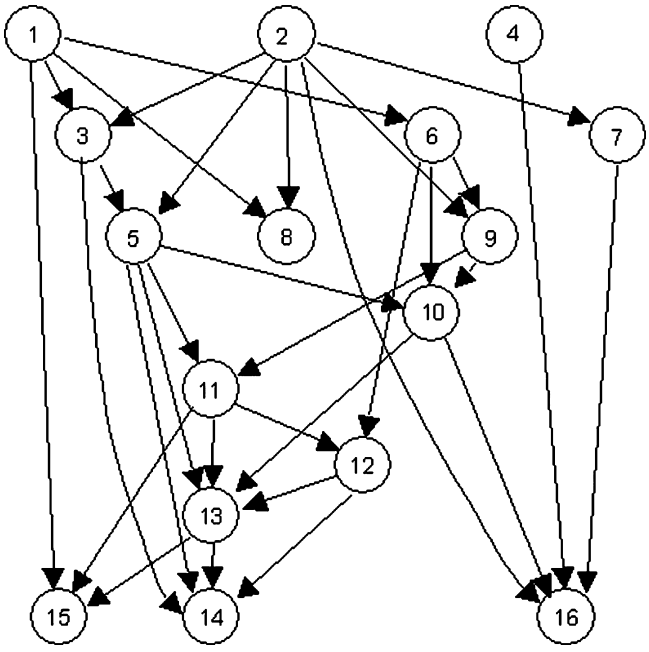

Fig. 11. Bayesian network structure applying the MCMC algorithm.

4.4. Improving the network structure

In practice, the search-and-score algorithms are not exact, and used only as initial approximations. Also, since the K2 and MCMC algorithms applied different tradeoffs for searching the structure, those algorithms can produce different results. But both structures can be considered on the resulting network structure. To improve the network structure, the following steps are executed:

- fusion of the results applying the K2 and MCMC algorithms;
- groups of variables are arranged in layers;
- constraint-based conditions and knowledge are applied.

The fusion of the results applying K2 and MCMC basically confirms the edges present in both structures (Figs. 10 and 11) and submits the remaining edges to erasing based on constrains and domain knowledge.

For a better understanding of the relationship among variables, those are separated in several layers. In this structure, three layers are considered: fault causes, pattern recognition, and sensors. Fault causes are the possible causes of faults such as faults in the air fan (aF), faults in the refrigeration system (rF), growth of J_n, and low H_2 pressure (see Sections 3.1–3.4). Sensors are variables that can easily be monitored using sensors (such as output voltage$_{stack}$ V, electrical current I_{FC}, temperature T, power, and H_2 pressure). Pattern recognition is associated with variables difficult to monitor in a real machine, but that play an important role in a cause-effect structure and define a fault pattern.

Some of the constraints to be considered are: (1) independent fault cause assumption, i.e. only one fault takes place each time, and one fault cause does not influence other fault cause; (2) independent sensors—edges among sensors can be erased because their values are always observed.

After that, domain knowledge is applied; basically, the submitted edges are compared with the relationship among variables in the process. For example, an edge from variable 7 (stoichiometry) to variable 16 (pH_2) appears in Fig. 11 (applying MCMC) but not in Fig. 10 (applying K2), then this is one of the edges submitted to be erased. According to Fig. 7, a variation of the pH_2 does not have a significant influence in the stoichiometry, then is concluded that this edge does not match the process evolution and, therefore, the edge is erased. A similar process is applied for all the remaining edges.

Fig. 12 illustrates the resulting Bayesian structure.

4.5. Conditional probability estimation

The probabilities in Bayesian networks are represented by CP objects (CP = conditional probability), which define the probability distribution of a node given its parents. When all nodes contain discrete values, a CP object can be described as a table.

Table 2 presents the CP obtained by the maximum posteriori likelihood algorithm [15] on the network structure considered in Fig. 12. Note that the probabilities of nodes 1–4, correspond to prior probabilities (i.e. nodes 1–4 do not have parents), and

Table 2
Conditional probabilities of the Bayesian network (F = false, T = true)

node J_n
F: 0.7465
T: 0.2535

node rF
F: 0.7490
T: 0.2510

node Flow
F F: 1.0000 0.0000
T F: 0.0000 1.0000
F T: 0.6829 0.3171
T T: 0.0000 0.0000

node λ
F: 0.9697 0.0303
T: 0.2469 0.7531

node Drying
F: 0.9794 0.0206
T: 0.2777 0.7223

node Overld
F: 0.7728 0.2272
T: 0.7607 0.2393

node I_{FC}
F F F: 0.6550 0.3450
T F F: 0.4946 0.5054
F T F: 0.9000 0.1000
T T F: 0.0000 0.0000
F F T: 0.9689 0.0311
T F T: 0.0582 0.9418
F T T: 0.9298 0.0702
T T T: 0.0000 1.0000

node Power
F: 0.9872 0.0128
T: 0.7565 0.2435

node aF
F: 0.7572
T: 0.2428

node H_2
F: 0.7473
T: 0.2527

node Q_{gen}
F F: 0.8029 0.1971
T F: 0.0681 0.9319
F T: 0.8123 0.1877
T T: 0.0000 0.0000

node Flood
F: 0.9119 0.0881
T: 0.0014 0.9986

node HR_{out}
F F: 0.8467 0.1533
T F: 0.9000 0.1000
F T: 0.0000 1.0000
T T: 0.0000 0.0000

Table 2 (*Continued*)

node Volt
F: 0.9637 0.0363
T: 0.8113 0.1887

node *T*
F: 1.0000 0.0000
T: 0.7604 0.2396

node pH_2
F: 1.0000 0.0000
T: 0.0000 1.0000

the probabilities of nodes 5, 6, . . ., 16 correspond to conditional probabilities.

The Bayesian network B composed of the network structure $\mathcal{G}$ plus conditional probabilities CP is ready to be used for fault diagnosis in a PEMFC. An inference is the computation of a conditional probability $p(X_q|X_E)$, where X_q is the variable of interest (e.g. the most probable fault cause) and X_E is the variable, or set of variables that have been observed (i.e. the effects observed by sensors).

There are many different algorithms for calculating the inference in Bayesian networks, which apply different tradeoffs between speed, complexity, generality, and accuracy [15]. The variable elimination algorithm permits the inference calculation on a Bayesian network with a generic structure. The JavaBayes System [8] implements this algorithm on a graphic interface. Figs. 13 and 14 illustrate the utilization of this program for the inference calculation for fault diagnosis in PEMFCs. Fig. 13 depicts the graphical representation of the Bayesian structure. In this case, electrical current I_{FC} and temperature T are the evidence observed (i.e. $I_{FC} = 1$ and $T = 1$ indicate a type of abnormal situation). In Fig. 14, the conditional probabilities have been calculated for all fault causes (J_n, aF, rF and H_2). In this case, when $I_{FC} = 1$ and $T = 1$ the most probable fault cause is aF (reduction in air flow) with 74% probability. The causes rF and J_n have intermediary probabilities, 39% and 34%, respectively. And cause H_2 has the least probability, 4%.

Several tests have been conducted to verify the effectiveness of the diagnosis; in all tests performed, the diagnosis always indicated the true cause as the most probable one [16].

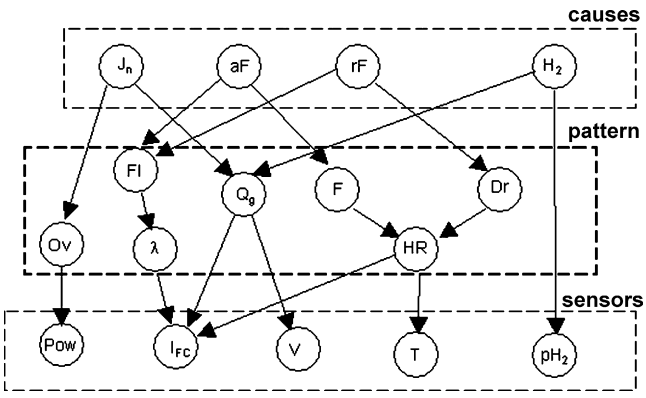

Fig. 12. Network structure for fault diagnosis in a PEMFC.

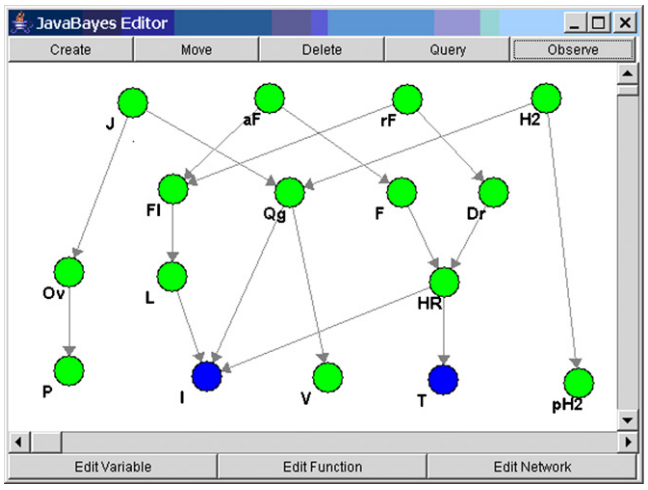

Fig. 13. Bayesian structure in the JavaBayes system.

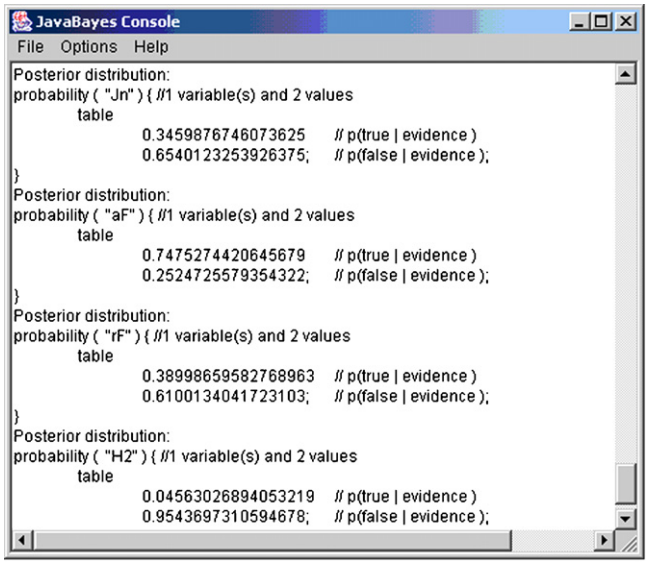

Fig. 14. Inference calculation in the JavaBayes system.

Network structures representing a diagnostic process play a fundamental role for fault tolerant machines since they can be associated with fault treatment processes (i.e. performing the fault diagnosis to identify the fault cause and executing the automatic recovery process). In [18] and [17] the fault detection and fault treatment by automatic recovery processes in electric autonomous guided vehicles (AGV) and machining processes have been analyzed.

5. Conclusion

The construction of a network structure for fault diagnosis in proton exchange membrane fuel cells (PEMFC) was executed implementing probabilistic approaches.

Fault records of some variables were constructed including variables difficult to monitor on a real machine. The record of all relevant variables is essential for the construction of the network

structure avoiding hidden variables, especially on intermediary layers.

For the construction of a network structure, the sole implementation of probabilistic approaches (such as the K2 and MCMC algorithms), is not enough for the construction of a "good" network, as presented in Figs. 10 and 11. An understanding of the process (e.g. processes in PEMFCs), is recommended, particularly for applying constrain-based conditions and knowledge to improve the network structure.

For the diagnostic process (i.e. the inference calculation), the evidence was based on observations of variables that can be easily monitored by sensors like voltmeters, ammeters, thermocouples, etc. This allows an easy implementation of fault diagnostic processes in FC systems.

The tests have shown agreement between the inference results and the original fault causes. They will allow the implementation of an on-line supervisor for fault diagnosis applying Bayesian networks constructed as described in this research.

Topics such as the study of fault effects in FCs, the construction of network structures for fault diagnosis in FCs, and their association to fault treatment processes are still under study, and are still open to research contributions.

Acknowledgment

The authors thank FAPESP, CNPq, and CAPES for the financial support to the present project, and Prof. J.M. Correa and Prof. F.G. Cozman for academic contribution.

References

[1] P.A.C. Chang, J. St-Pierre, J. Stumper, B. Wetton, J. Power Sources 162 (1) (2006) 340–355.
[2] D.M. Chickering, J. Mach. Learn. Res. 3 (2002) 507–554.
[3] C.F. Chien, S.L. Chen, Y.S. Lin, IEEE Trans. Power Deliv. 17 (3) (2002) 785–793.
[4] G.F. Cooper, E. Herskovits, Mach. Learn. 9 (1992) 309–347.
[5] J.M. Correa, F.A. Farret, L.N. Canha, M.G. Simoes, V.A. Popov, IEEE Trans. Energy Conver. 20 (1) (2005) 211–218.
[6] J.M. Correa, F.A. Farret, L.N. Canha, M.G. Simoes, IEEE Trans. Ind. Electron. 51 (5) (2004) 1103–1112.
[7] J.M. Correa, F.A. Farret, J.R. Gomes, M.G. Simoes, IEEE Trans. Ind. Appl. Soc. 39 (4) (2003) 1136–1142.
[8] F.G. Cozman, http://www-2.cs.cmu.edu/~javabayes/ (2001).
[9] N. Fouquet, C. Doulet, C. Nouillant, G. Dauphin-Tanguy, B. Ould Bouamama, J. Power Sources 159 (2) (2006) 905–913.
[10] S.A. Freunberger, M. Santis, I.A. Schneider, A. Wokaun, F.N. Büchi, J. Electrochem. Soc. 153 (2) (2006), A396–A405 & A909–A913.
[11] J. Larminie, A. Dicks, Fuel Cell Systems Explained, John Wiley & Sons Ltd., 2003.
[12] U. Lerner, B. Moses, M. Scott, S. McIlraith, D. Koller, Proceedings of 18th Conference on Uncertainty in AI, 2002, pp. 301–310.
[13] K. Murphy, (2005). http://bnt.sourceforge.net/.
[14] J. Pearl, Causality: Models Reasoning and Inference, Cambridge University Press, 2000.
[15] J. Pearl, Probabilistic Reasoning in Intelligent Systems: Networks of Plausible Inference, Morgan Kaufmann Publ., 1988.
[16] L.A.M. Riascos, M.G. Simoes, F.G. Cozman, P.E. Miyagi, Proceedings of the 41st IEEE-IAS, Industry Application Society, Tampa-FL, USA, 2006.
[17] L.A.M. Riascos, P.E. Miyagi, Cont. Eng. Pract. 14 (2006) 397–408.
[18] L.A.M. Riascos, F.G. Cozman, P.E. Miyagi, Detection and treatment of faults in automated machines based on Petri nets and Bayesian networks, in: Proceedings of IEEE-ISIE (International Symposium in Industrial Electronics), Rio de Janeiro, Brazil, 2003.
[19] M. Santis, S.A. Freunberger, M. Papra, A. Wokaun, F.N. Büchi, J. Power Sources 161 (2) (2006) 1076–1083.